RAPID COMMUNICATIONS

PHYSICAL REVIEW E VOLUME 53, NUMBER 2 FEBRUARY 1996

Chaotic spatially subharmonic oscillations

D. Lima, A. De Wit,* G. Dewel, and P. Borckmans

Service de Chimie Physique and Centre for Nonlinear Phenomena and Complex Systems, Code Postal 231, Université Libre de Bruxelles, Campus Plaine, 1050 Brussels, Belgium

(Received 5 October 1995)

The interplay between two instabilities respectively breaking space and time symmetries can give rise to spatially subharmonic oscillations generated by a self-induced parametric instability. In one-dimensional systems, the resulting dynamics consists in a pattern with two wave numbers oscillating with one frequency. Conditions are given for which this solution becomes phase unstable giving rise to spatiotemporal chaos.

PACS number(s): 05.45.+b, 47.20.Ky

A rich variety of complex spatiotemporal behaviors may occur in the vicinity of multiple bifurcation points [1]. In particular, the interaction between a steady instability that breaks spatial symmetry and a bifurcation breaking time translation symmetry has been the subject of numerous studies [2–7]. As an example, we have reported previously that the interplay between the Turing and Hopf instabilities can give rise to localized structures in the form of asynchronous wave sources with structured cores [8] or to a chaotic Turing-Hopf mixed mode [9]. Such dynamical behaviors have now been observed experimentally in a chemical system [8,10]. In this Rapid Communication, we show that self-induced subharmonic bifurcations can also be generated by resonances near such degenerate instability points. In some cases, the resulting subharmonic dynamics can become spatiotemporally chaotic.

We suppose that the reference homogeneous steady state (HSS) of a one-dimensional (1D) physicochemical system can undergo both a pattern-forming instability giving rise to a periodic structure with a wavelength $\lambda_c = 2\pi/q_c$ and a Hopf bifurcation. The distance between the two thresholds of instability, the unfolding parameter, is denoted as δ. For example, in the case of chemical reactions taking place in a gel, the concentration of the color indicator immobilized in the matrix allows one to control the distance between the Turing and Hopf bifurcation points [8,10]. If δ is sufficiently small, the eigenvalue of the 1/2 subharmonic of the steady critical mode can become complex and near the critical point the corresponding real part is small. The resonant interaction between the corresponding pair of Hopf modes with wave number $q_c/2$ and the steady state with wave number q_c must then be taken into account [11]. In the vicinity of such a critical situation, the field variable of the problem $\underline{C}(x,t)$ may be expressed in terms of the steady mode with amplitude T and two traveling waves with amplitudes A_R and A_L:

$$\underline{C}(x,t)=\underline{C}_0+Te^{iq_cx}\underline{e}_T+A_Le^{i[\omega(q_c/2)t+q_cx/2]}\underline{e}_L +A_Re^{i[\omega(q_c/2)t-q_cx/2]}\underline{e}_R+\text{c.c.} \quad (1)$$

where $\underline{C}_0$ is the reference HSS, $\underline{e}_T$, $\underline{e}_L$, and $\underline{e}_R$ the critical eigenvectors of the linearized matrix corresponding to the steady state and the Hopf modes while $\omega(q_c/2)$ is the critical frequency of the Hopf mode with wave number $q_c/2$. The competition between these modes is then described by amplitude equations that are derived by the use of standard techniques [12,13]. If τ and χ are the slow time and space scales then

$$\frac{\partial T}{\partial \tau}=\mu_T T-g|T|^2T-\lambda(|A_R|^2+|A_L|^2)T+\upsilon A_R^*A_L+D\frac{\partial^2 T}{\partial \chi^2}, \quad (2)$$

$$\frac{\partial A_R}{\partial \tau}=\mu' A_R-g'|A_R|^2A_R-h'|A_L|^2A_R-\lambda'|T|^2A_R +\upsilon' T^*A_L-c\frac{\partial A_R}{\partial \chi}+D'\frac{\partial^2 A_R}{\partial \chi^2}, \quad (3)$$

$$\frac{\partial A_L}{\partial \tau}=\mu' A_L-g'|A_L|^2A_L-h'|A_R|^2A_L-\lambda'|T|^2A_L+\upsilon' TA_R +c\frac{\partial A_L}{\partial \chi}+D'\frac{\partial^2 A_L}{\partial \chi^2}. \quad (4)$$

The coupling constants appearing in these equations can be related to the parameters of the system. The primed coefficients are complex ($\alpha'=\alpha_r'+i\alpha_i'$) while $\mu_r'=\mu_T+\delta$ where μ_T measures the distance from the steady bifurcation threshold and c is related to the group velocity of the waves. The most important feature of the above equations is the presence of a resonant interaction proportional to υ and υ' induced by the coupling between the steady mode and the waves. This term introduces a phase dependence into the dynamics. The simplest nontrivial solution of these equations is a pure steady state:

$$T^2=\frac{\mu_T}{g}, \quad A_R=A_L=0. \quad (5)$$

It is the first to appear supercritically when $\delta<0$ and $g>0$. As the bifurcation parameter μ_T is increased above zero, this periodic structure undergoes an instability for $\mu_T=\mu_I$ where μ_I is determined from

*Electronic address: adewit@ulb.ac.be

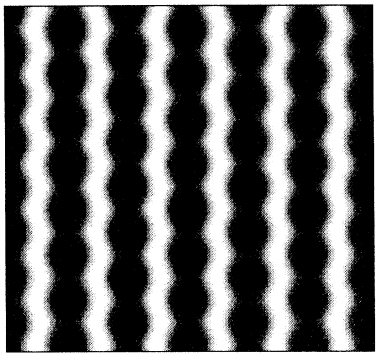

FIG. 1. Space-time density plot of $C(x,t)$ showing the stable subharmonic mixed mode. The amplitudes T, A_R, and A_L have been obtained by integrating the system (2)–(4) without diffusion and group velocity using an explicit Euler scheme. The parameters are $\mu_T=0.7$, $g=2$, $\lambda=4$, $v=1$, $\delta=-0.05$, $g'=3+i$, $h'=6+i$, $\lambda'=2+i$, $v'=0.2+0.5i$. The field variable is then reconstructed as $C(x,t)=Te^{i0.4x}+A_Le^{i(0.1t+0.2x)}+A_Re^{i(0.1t-0.2x)}+\text{c.c.}$ The minima (maxima) of $C(x,t)$ are in white (black). Time is running downwards.

$$\mu_I+\delta-\lambda_r'(\mu_I/g)+v_r'\sqrt{\mu_I/g}=0 \tag{6}$$

obtained through a linear stability analysis. When the following condition is satisfied:

$$2(g_r'+h_r')\mu_I-[v_r-2\lambda_r\sqrt{\mu_I/g}][v_r'-2\lambda_r'\sqrt{\mu_I/g}]>0, \tag{7}$$

the solution that bifurcates from the pure steady state mode at $\mu_T=\mu_I$ corresponds to a mixed mode for which

$$T=T_M, \quad A_R=R_Me^{i[\Omega_Mt+\phi_R]}, \quad A_L=R_Me^{i[\Omega_Mt+\phi_L]}. \tag{8}$$

By an appropriate choice of the origin of coordinates, we can consider T_M as real. When $v_r'>0$, the phase dynamics implies that

$$\phi_R=\phi_L. \tag{9}$$

Substituting into Eqs. (2)–(4), and equating real and imaginary parts, we get

$$\Omega_M=\mu_i'-R_M^2[g_i'+h_i']-\lambda_i'T_M^2+v_i'T_M, \tag{10}$$

$$R_M^2=\frac{\mu_r'-\lambda_r'T_M^2+v_r'T_M}{[g_r'+h_r']}, \tag{11}$$

$$0=[\mu_T-2\lambda R_M^2]T_M+vR_M^2-gT_M^3. \tag{12}$$

The spatiotemporal dynamics corresponding to this mixed mode solution is thus the combination of a steady structure with wavelength q_c and a standing wave formed by the superposition of the left- and right-going waves ($A_R=A_L$) with wave number $q_c/2$ and frequency $\omega(q_c/2)$. The corresponding space-time plot for the reconstructed field $C(x,t)$[Eq. (1)] is displayed in Fig. 1. The characteristic polygonal space-time structure of a mixed mode is obtained. At each location, the system is oscillating with one frequency but, because of the presence of two wave numbers, we see that the minima of the structure are shifted one wavelength every half period of oscillation. This dynamical behavior presents strong analogies with the spatially subharmonic oscillations

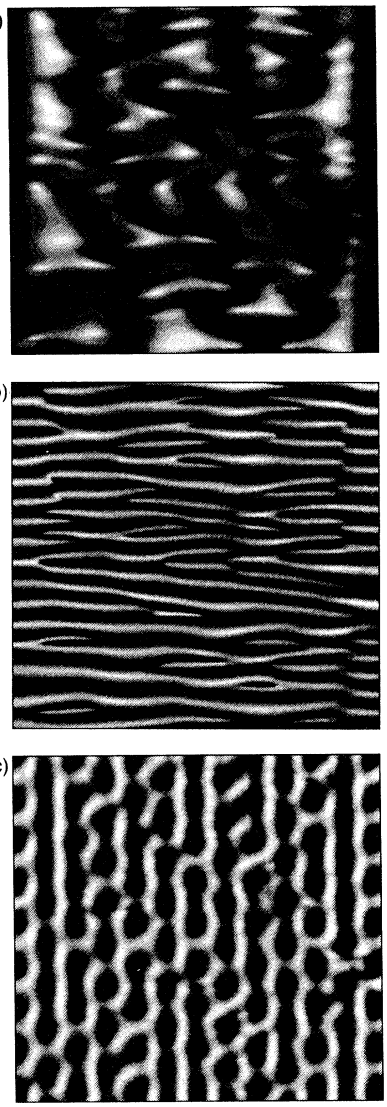

FIG. 2. Space-time density plots of the spatiotemporal chaos obtained when the subharmonic mixed mode is phase unstable. Integration of the amplitude equations (2)–(4) is performed with diffusion and group velocity on a system of length 64 during 120 units of time using periodic boundary conditions. The spatial differentiation has been made using finite differences. All conditions are the same as in Fig. 1 except $g'=3.0+0.2i$, $\lambda'=2+5i$, $D=0$, $D'=0.5+5i$ while $c=0.01$. (a) and (b) amplitude and phase of the right-going wave shown on scales τ and χ; (c) field variable $C(x,t)=Te^{i0.3x}+A_Le^{i(0.1t+1.5x)}+A_Re^{i(0.1t-1.5x)}+\text{c.c.}$ reconstructed on scales t and x.

that have been observed on the 1D front in the flow of a fluid inside a partially filled rotating horizontal cylinder [14]. Similar oscillating patterns have also been obtained in numerical integration of a reaction-diffusion model in the vicinity of the codimension-two Turing-Hopf point [15]. These mixed modes are of a different origin than those introduced in [4]. It is worthwhile to point out that for the values of the parameters used in Fig. 1, the standing wave of the system [(3) and (4)] with $T=0$ are unstable versus traveling waves ($h_r'>g_r'$). It is known that such a standing wave can be stabilized if an external time modulation with a frequency twice the frequency of the traveling waves is applied to the system [16,17]. Here we show that the stabilization of the standing waves can also be self-induced by an intrinsic coupling with the steady mode which plays the role of an external forcing by restoring the left-right symmetry.

The mixed mode [Eq. (8)] is stable versus spatially uniform amplitude perturbations as long as the following inequalities are satisfied:

$$\Delta=[g_r'+h_r']\left[2gT_M^2+\frac{vR_M^2}{T_M}\right]-[v_r'-2\lambda_r'T_M][v-2\lambda T_M]>0, \tag{13}$$

$$Tr=-\left[2(g_r'+h_r')R_M^2+2gT_M^2+\frac{vR_M^2}{T_M}\right]<0. \tag{14}$$

However, in the experiments on 1D fronts [14], when the bifurcation parameter is increased beyond μ_I, spatial modulations appear spontaneously which disturb the regularity of this oscillating subharmonic pattern. It is thus necessary to study also the stability of the mixed mode with respect to inhomogeneous perturbations. The mixed mode solution [Eq. (8)] is invariant under the transformation

$$\psi(T, A_L, A_R)=(T,e^{i\psi}A_L,e^{i\psi}A_R) \tag{15}$$

which corresponds to a shift in time $t'\rightarrow t-\psi/\Omega_M$. This property generates a whole family of solutions and induces a zero eigenvalue in the homogeneous linearized matrix. In the presence of slow spatial modulations that preserve the condition (9) on the large scales, $\psi(x,t)$ depends on space and time and obeys a phase diffusion equation of the form [12]

$$\frac{\partial\psi}{\partial t}=\mathscr{D}\frac{\partial^2\psi}{\partial x^2}+\kappa\left(\frac{\partial\psi}{\partial x}\right)^2. \tag{16}$$

A phase instability occurs when $\mathscr{D}=0$. After a little algebra, it is easy to show that this long wavelength instability takes place when

$$\mathscr{D}=D_r'+\frac{D_i'}{\Delta}\left\{[g_i'+h_i']\left[2gT_M^2+\frac{vR_M^2}{T_M}\right]-[v_i'-2\lambda_i'T_M][v-2\lambda T_M]\right\}<0. \tag{17}$$

This condition is the analog for the subharmonic mixed mode of the Benjamin-Feir stability criterion for the traveling waves [12]. We have numerically integrated the amplitude equations (2)–(4) for values of parameters that satisfy the condition (17). In the case presented here, the resulting phase instability spontaneously generates numerous phase defects [18] and large fluctuations of the three amplitudes thus mediating spatiotemporal chaos as shown in Fig. 2. When the amplitude of the waves locally reaches zero [white regions in Fig. 2(a)], the phase of the waves exhibits space-time dislocations [Fig. 2(b)], a behavior reminiscent of the so-called "amplitude chaos" [18,19]. The space-time plot of the reconstructed field variable $\underline{C}(x,t)$ confirms that the system does not oscillate at the locations where the amplitude of the waves is minimum thus expressing the steady state solution. On the contrary, when the amplitude of the waves is maximum, the amplitude of the steady state is minimum and the system is locally in an oscillating mode.

As long as the phase difference is locked on the large scale, i.e., condition (9) is fulfilled, the resonant interaction plays a crucial role in the localization of the defects [17]. However, when the group velocity is sufficiently large, the state with $\Phi=\phi_R-\phi_L=0$ is destabilized. The phase variable Φ then obeys a sine-Gordon equation of diffusion type that is known to admit stable propagating solitons as solutions [20,21]. Such solitary waves have also been observed in the film draining experiment [22].

In this Rapid Communication, we have shown that the coupling between a pattern-forming instability and a Hopf instability can induce a bifurcation from a steady pattern towards a subharmonic structure characterized by two wave numbers and one frequency. We have next given the conditions under which this subharmonic pattern can become phase unstable giving rise to a spatiotemporally chaotic dynamics. This scenario explains the sequence of bifurcations recently observed experimentally in a hydrodynamical system [14]. Such a scenario should also exist in chemical systems where the degeneracy between the Turing and Hopf instabilities can be achieved experimentally. The subharmonic pattern has indeed been observed in the numerical integration of the reaction-diffusion Brusselator model near the codimension-two Turing-Hopf point [15]. Let us furthermore note that subharmonic patterns have also been obtained in a study of two different immiscible liquids lying in layers between horizontal walls and heated from below [23]. Finally, a parametric instability of a homogeneous limit cycle towards a subharmonic mixed mode with two wave numbers and two frequencies followed by a transition to spatiotemporal chaos has also been documented recently in the Brusselator model [15] and in the Gray-Scott model [24]. In the latter case, the stabilization of the spatiotemporal chaos has allowed one to track an unstable Turing pattern. These results emphasize the need to understand in detail the mechanisms of appearance of spatiotemporal chaos near degenerate bifurcation points.

D.L. thanks the CNPQ (Brazil) for its financial support. A.D., G.D., and P.B. acknowledge financial help from the F.N.R.S. (Belgium).

[1] J. Guckenheimer and P. Holmes, *Nonlinear Oscillations, Dynamical Systems, and Bifurcations of Vector Fields* (Springer Verlag, New York, 1983).
[2] J.P. Keener, Stud. Appl. Math. **55**, 187 (1976).
[3] H. Kidachi, Prog. Theor. Phys. **63**, 1152 (1980).
[4] B.J.A Zielinska, D. Mukamel, and V. Steinberg, Phys. Rev. A **33**, 1454 (1986), and references therein.
[5] W. Zimmermann, D. Armbruster, L. Kramer, and W. Kuang, Europhys. Lett. **6**, 505 (1988) and references therein.
[6] P. Kolodner, Phys. Rev. E **48**, R665 (1993).
[7] G. Heidemann, M. Bode, and H.-G. Purwins, Phys. Lett. A **177**, 225 (1993).
[8] J.-J. Perraud, A. De Wit, E. Dulos, P. De Kepper, G. Dewel, and P. Borckmans, Phys. Rev. Lett. **71**, 1272 (1993).
[9] A. De Wit, G. Dewel, and P. Borckmans, Phys. Rev. E **48**, R4191 (1993).
[10] P. De Kepper, J.-J. Perraud, B. Rudovics, and E. Dulos, Int. J. Bif. Chaos **4**, 1215 (1994).
[11] A. Hill, and I. Stewart, Dynam. Stab. Syst. **6**, 149 (1991).
[12] M.C. Cross and P.C. Hohenberg, Rev. Mod. Phys. **65**, 851 (1993).
[13] M. Cheng and H.-C. Chang, Phys. Fluids A **4**, 505 (1992).
[14] D.P. Vallette, W.S. Edwards, and J.P. Gollub, Phys. Rev. E **49**, R4783 (1994).
[15] A. De Wit, Ph.D. thesis, Université Libre de Bruxelles, 1993 (unpublished).
[16] H. Riecke, J.D. Crawford, and E. Knobloch, Phys. Rev. Lett. **61**, 1942 (1988).
[17] P. Coullet, K. Emilsson, and D. Walgraef, Physica D **61**, 132 (1992).
[18] P. Coullet, L. Gil, and J. Lega, Phys. Rev. Lett. **62**, 1619 (1989).
[19] B.I. Shraiman, A. Pumir, W. van Saarloos, P.C. Hohenberg, H. Chaté, and M. Holen, Physica D **57**, 241 (1992).
[20] M. Büttiker and R. Landauer, Phys. Rev. A **23**, 1397 (1981).
[21] Y. Tegami, Physica D **21**, 325 (1986).
[22] F. Melo and S. Douady, Phys. Rev. Lett. **71**, 3283 (1993).
[23] K. Fujimura and Y. Renardy, Physica D **85**, 25 (1995).
[24] V. Petrov, S. Métens, P. Borckmans, G. Dewel, and K. Showalter, Phys. Rev. Lett. **75**, 2895 (1995).

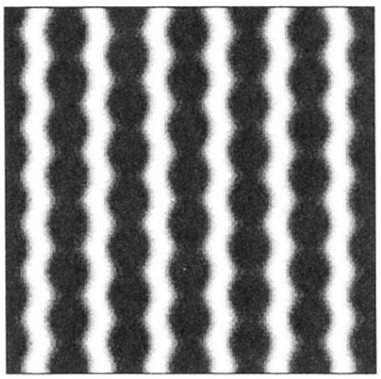

FIG. 1. Space-time density plot of $C(x,t)$ showing the stable subharmonic mixed mode. The amplitudes T, A_R, and A_L have been obtained by integrating the system (2)–(4) without diffusion and group velocity using an explicit Euler scheme. The parameters are $\mu_T=0.7$, $g=2$, $\lambda=4$, $v=1$, $\delta=-0.05$, $g'=3+i$, $h'=6+i$, $\lambda'=2+i$, $v'=0.2+0.5i$. The field variable is then reconstructed as $C(x,t)=Te^{i0.4x}+A_Le^{i(0.1t+0.2x)}+A_Re^{i(0.1t-0.2x)}+\text{c.c.}$ The minima (maxima) of $C(x,t)$ are in white (black). Time is running downwards.

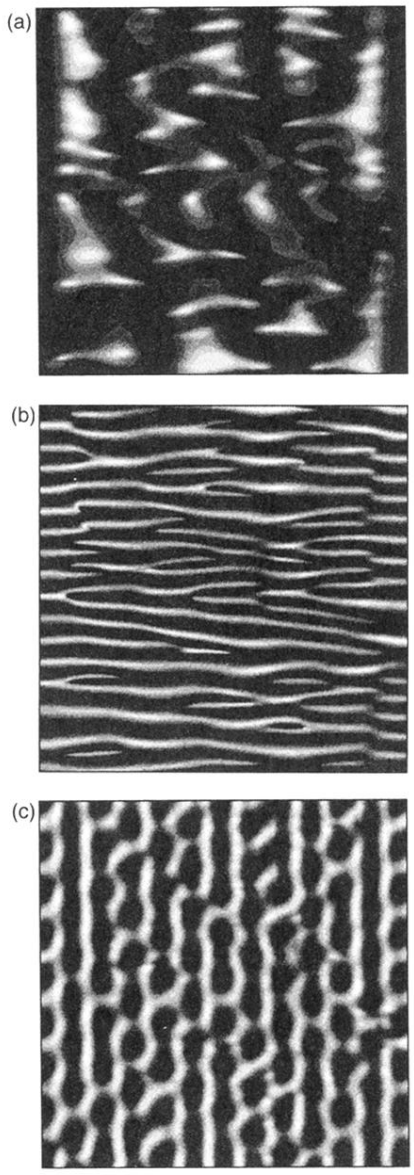

FIG. 2. Space-time density plots of the spatiotemporal chaos obtained when the subharmonic mixed mode is phase unstable. Integration of the amplitude equations (2)–(4) is performed with diffusion and group velocity on a system of length 64 during 120 units of time using periodic boundary conditions. The spatial differentiation has been made using finite differences. All conditions are the same as in Fig. 1 except $g'=3.0+0.2i$, $\lambda'=2+5i$, $D=0$, $D'=0.5+5i$ while $c=0.01$. (a) and (b) amplitude and phase of the right-going wave shown on scales τ and χ; (c) field variable $C(x,t)=Te^{i0.3x}+A_L e^{i(0.1t+1.5x)}+A_R e^{i(0.1t-1.5x)}+\text{c.c.}$ reconstructed on scales t and x.